Electronic Supplementary Information

Structural versatility and electronic structures of copper(I) thiocyanate (CuSCN)-ligand complexes

Pichaya Pattanasattayavong,*[ab] Daniel M. Packwood[c] and David J. Harding[d]

[a] Department of Materials Science and Engineering, School of Molecular Science and Engineering, Vidyasirimedhi Institute of Science and Technology (VISTEC), Rayong, 21210, Thailand

[b] Research Network of NANOTEC-VISTEC on Nanotechnology for Energy, Vidyasirimedhi Institute of Science and Technology (VISTEC), Rayong, 21210, Thailand

[c] Institute for Integrated Cell-Material Sciences (iCeMS), Kyoto University, Kyoto, 606-8501, Japan.

[d] Functional Materials and Nanotechnology Center of Excellence (FuNTech), Walailak University, Nakhon Si Thammarat, 80160, Thailand

* Corresponding author, email: pichaya.p@vistec.ac.th

This electronic supplementary information (ESI) contains: (1) structural drawings which display the interatomic short contacts of the 2D structures (Fig. S1); (2) electronic band structure and density of states (DOS) data calculated by density functional theory of all CuSCN-ligand complexes investigated in this work (Fig. S2-S29).

Electronic band structure: valence band (VB) states (light red lines) and maximum-energy VB points (red filled circles), conduction band (CB) from ligand states (light gray lines) and minimum-energy points (gray filled circles) which correspond to the fundamental band gaps, and CB from SCN states (light blue lines) and minimum-energy points (blue filled circles) which correspond to the Cu-SCN energy gaps.

Total and partial DOS: total DOS (thin black line), partial Cu 3*d* DOS (dark red lines), partial S 3*p* DOS (yellow lines), partial N 2*p* DOS (violet lines), and partial C 2*p* DOS (gray lines). The spectra are offset along the vertical axis, and the partial DOS of S, N, and C are multiplied by integers (indicated in the plots) for clarity.

For Fig. S2-S29, all plots are referenced to the top of the VB, at which point the energy is set to zero. The figures are arranged in the order of reducing Cu-SCN network dimensionality.

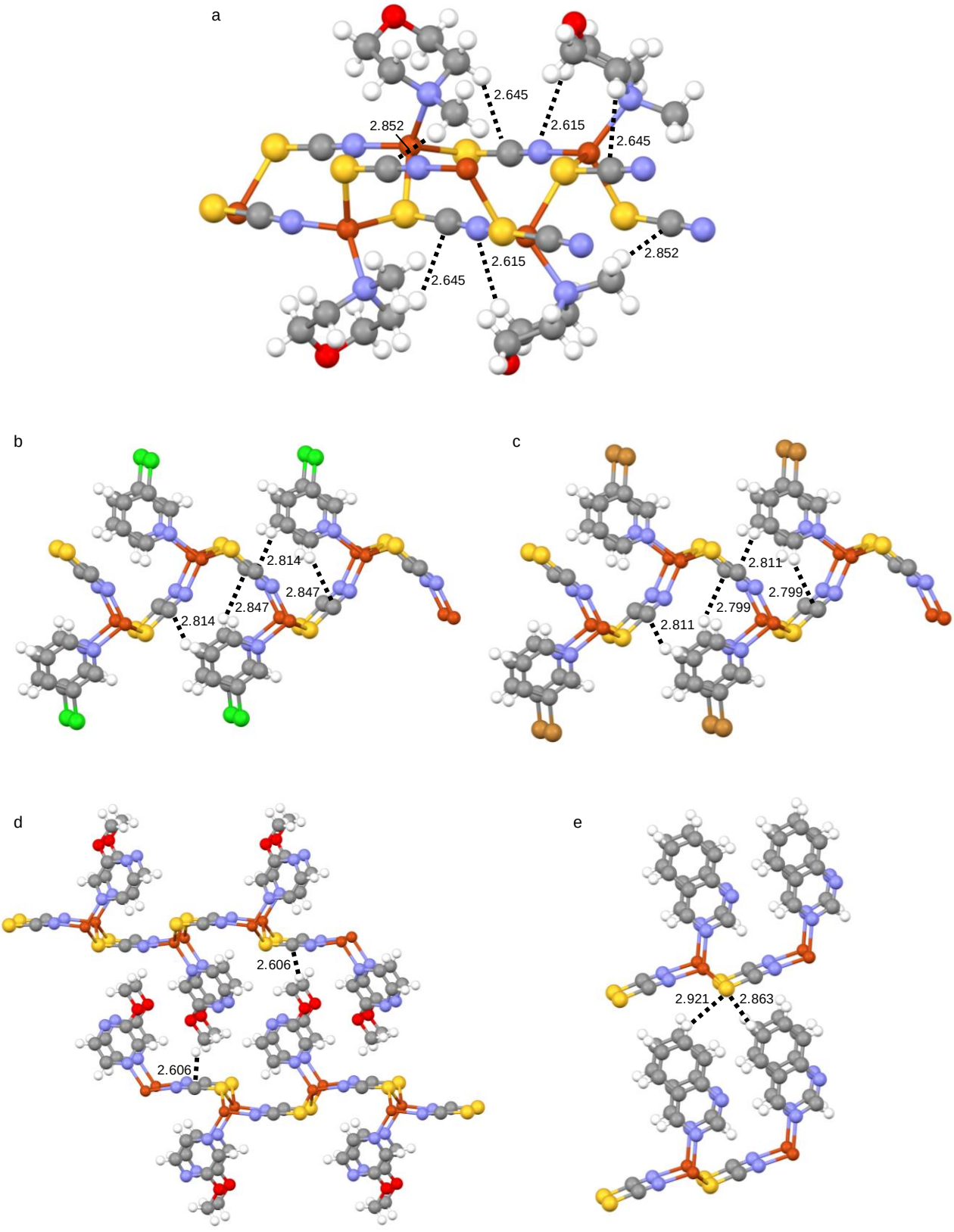

Fig. S1 Significant interatomic short contacts observed in the 2D structures. (a) Intralayer C-H···C contacts at 2.645 and 2.852 Å and intralayer C-H···N contacts at 2.615 Å in $[Cu(SCN)(4MeMorph)]_n$. (b) Intralayer C-H···C contacts at 2.814 and 2.847 Å in $[Cu(SCN)(3ClPy)]_n$. (c) Intralayer C-H···C contacts at 2.799 and 2.811 Å in $[Cu(SCN)(3BrPy)]_n$. (d) Interlayer C-H···C contacts at 2.606 Å in $[Cu(SCN)(2MeOPyz)]_n$. (e) Interlayer C-H···S contacts at 2.863 and 2.921 Å in $[Cu(SCN)(Qnz)]_n$. Color scheme: Cu = dark orange, S = yellow, C = gray, N = violet, H = white, O = red, Cl = green, and Br = brown.

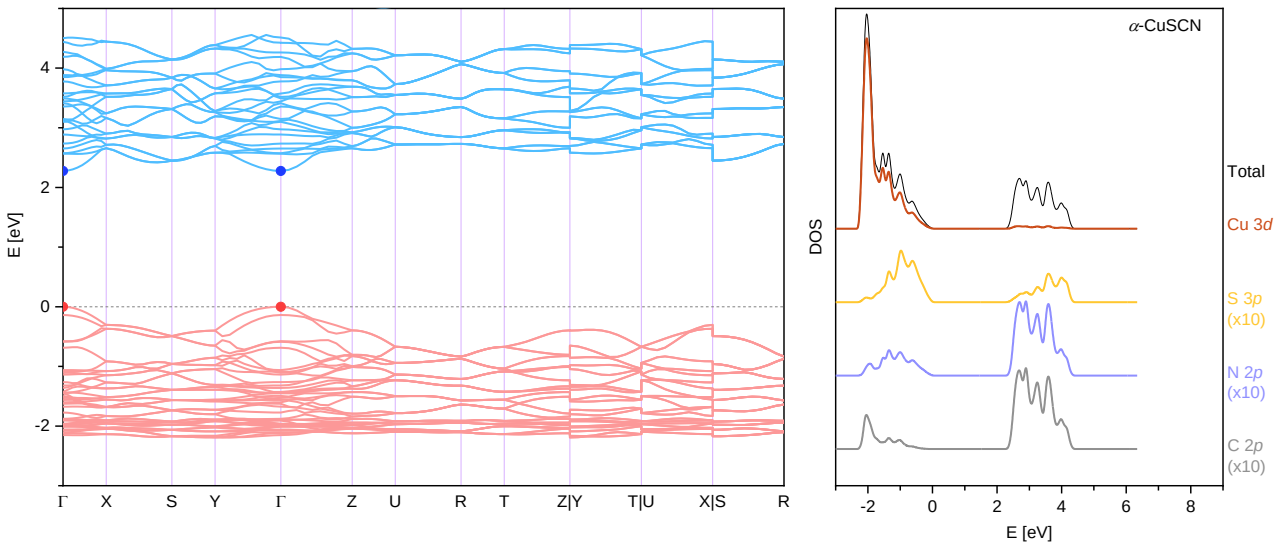

Fig. S2 Electronic band structure and DOS of 3D α-CuSCN.

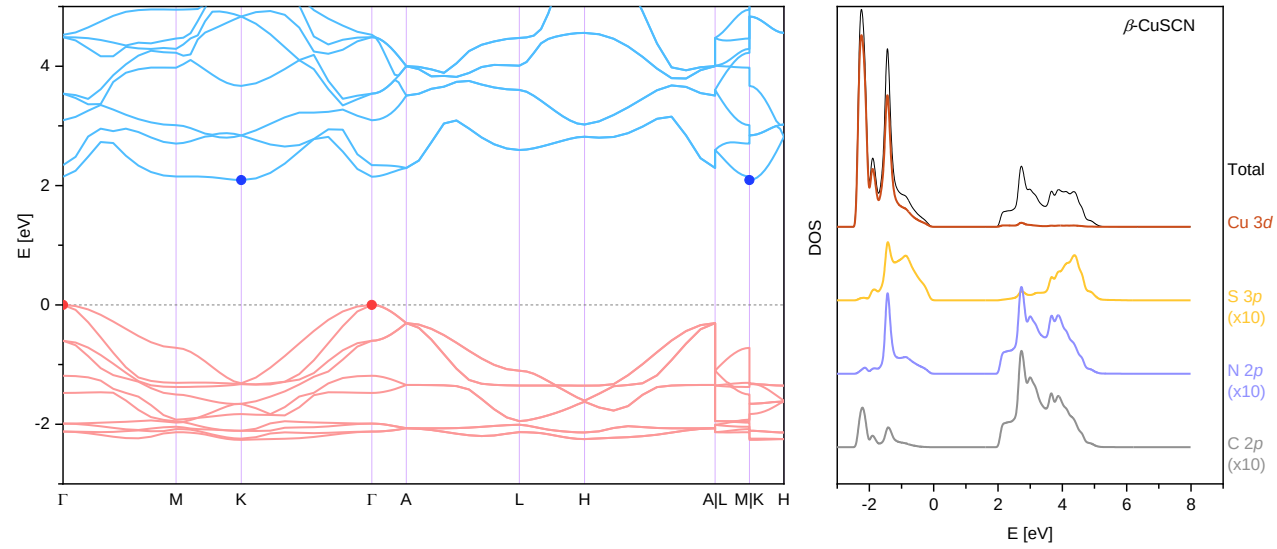

Fig. S3 Electronic band structure and DOS of 3D β-CuSCN.

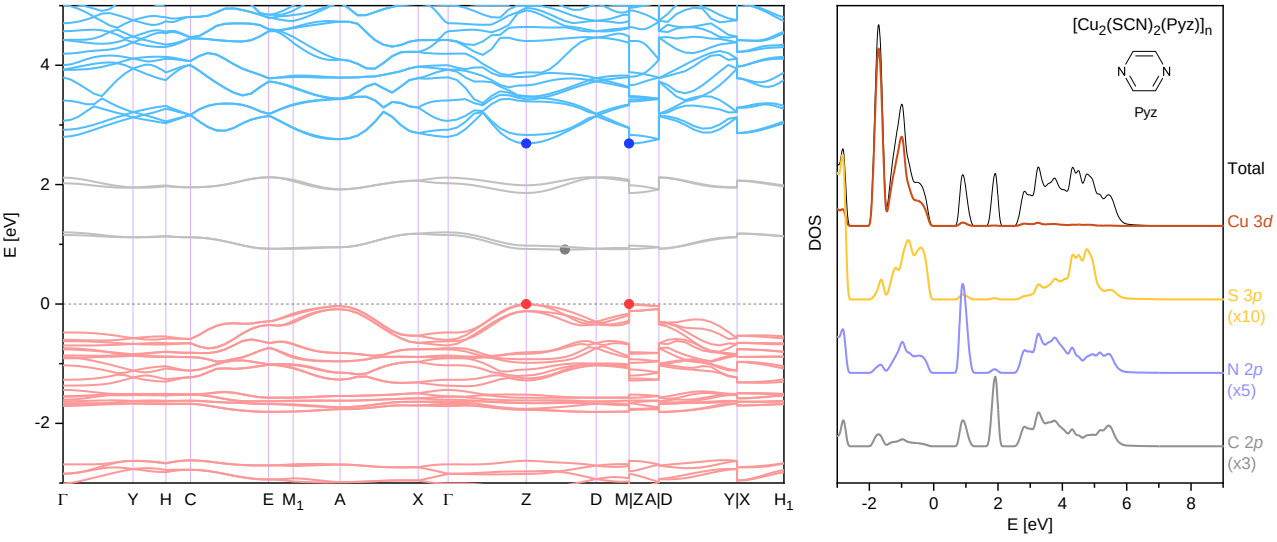

Fig. S4 Electronic band structure and DOS of bridged 2D $[Cu_2(SCN)_2(Pyz)]_n$.

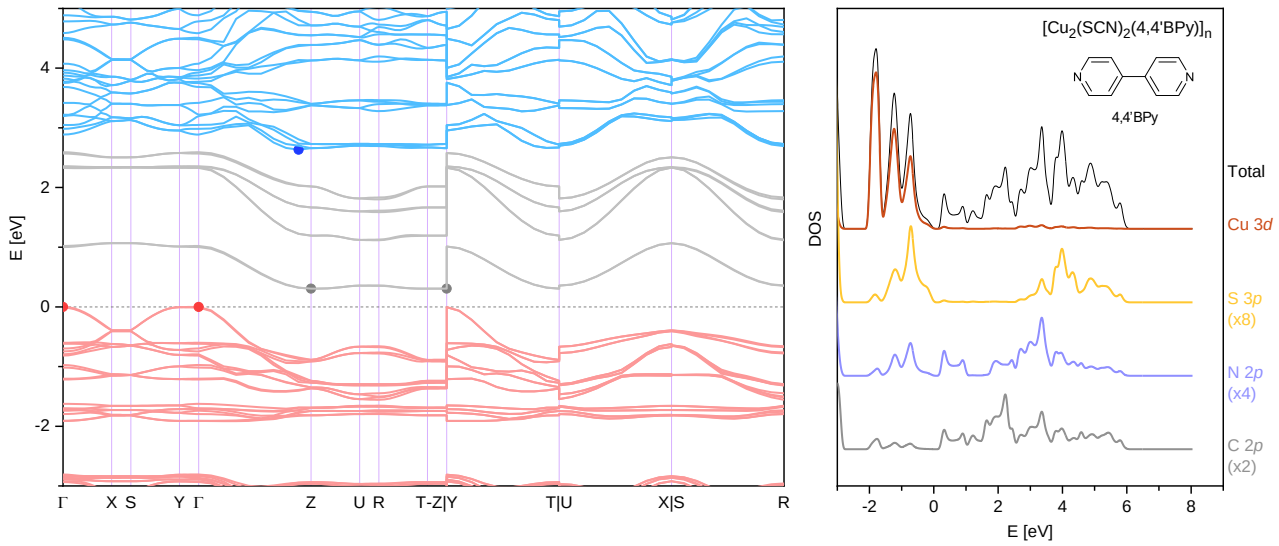

Fig. S5 Electronic band structure and DOS of bridged 2D $[Cu_2(SCN)_2(4,4'BPy)]_n$.

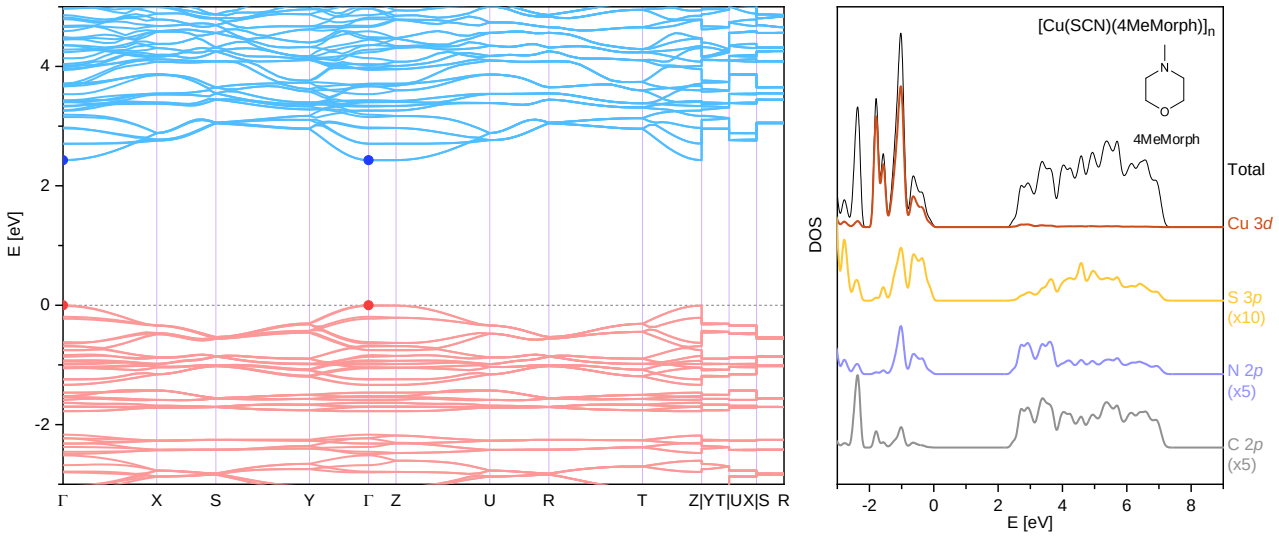

Fig. S6 Electronic band structure and DOS of 2D sheet $[Cu(SCN)(4MeMorph)]_n$.

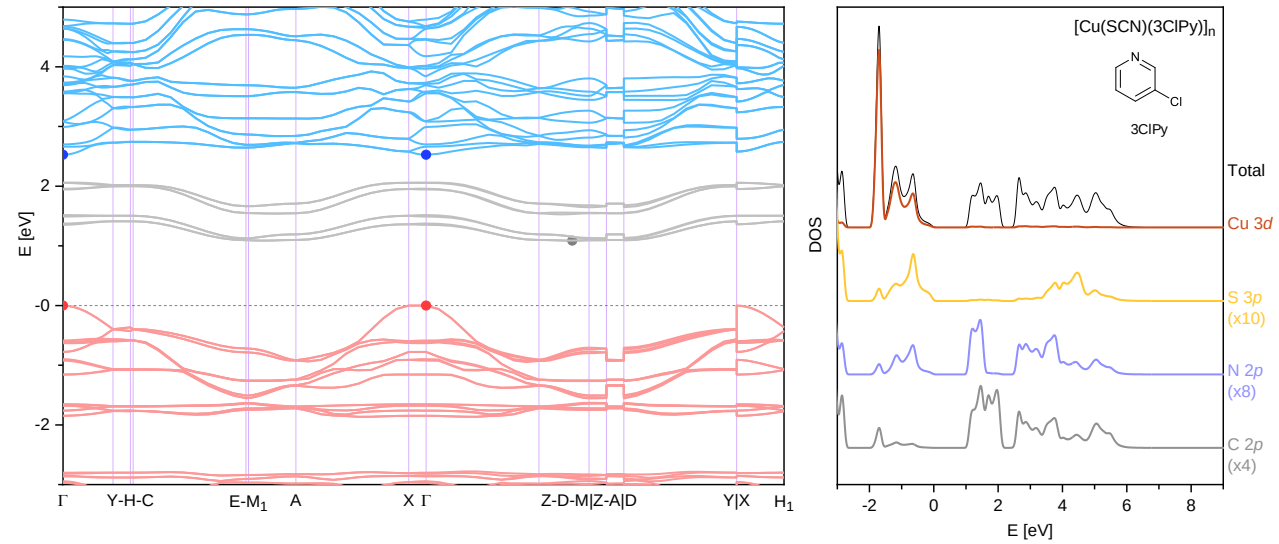

Fig. S7 Electronic band structure and DOS of 2D sheet $[Cu(SCN)(3ClPy)]_n$.

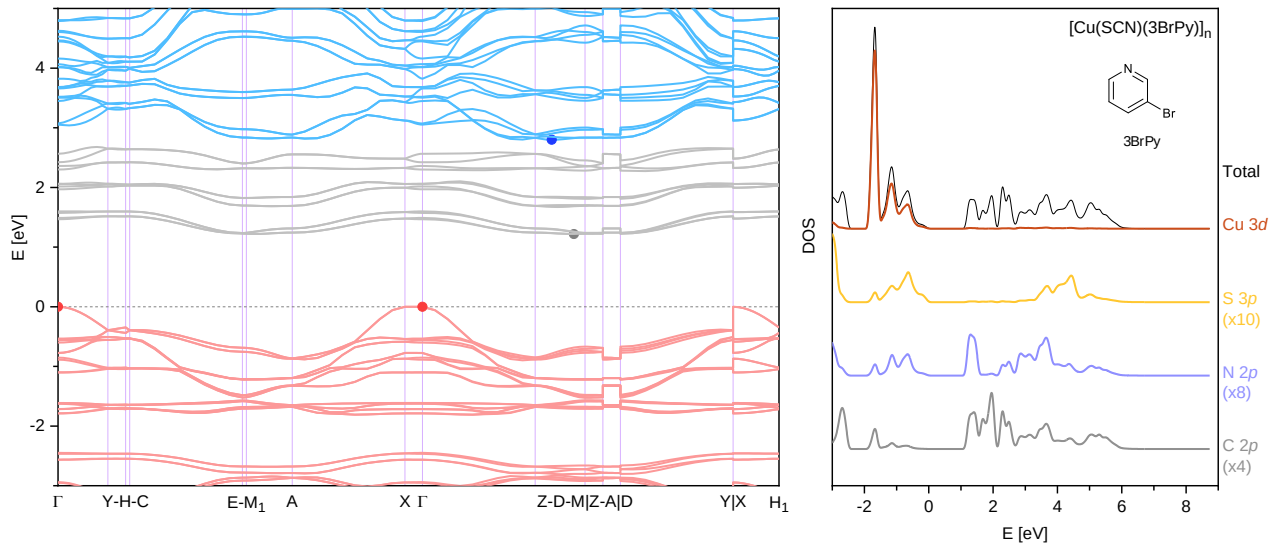

Fig. S8 Electronic band structure and DOS of 2D sheet $[Cu(SCN)(3BrPy)]_n$.

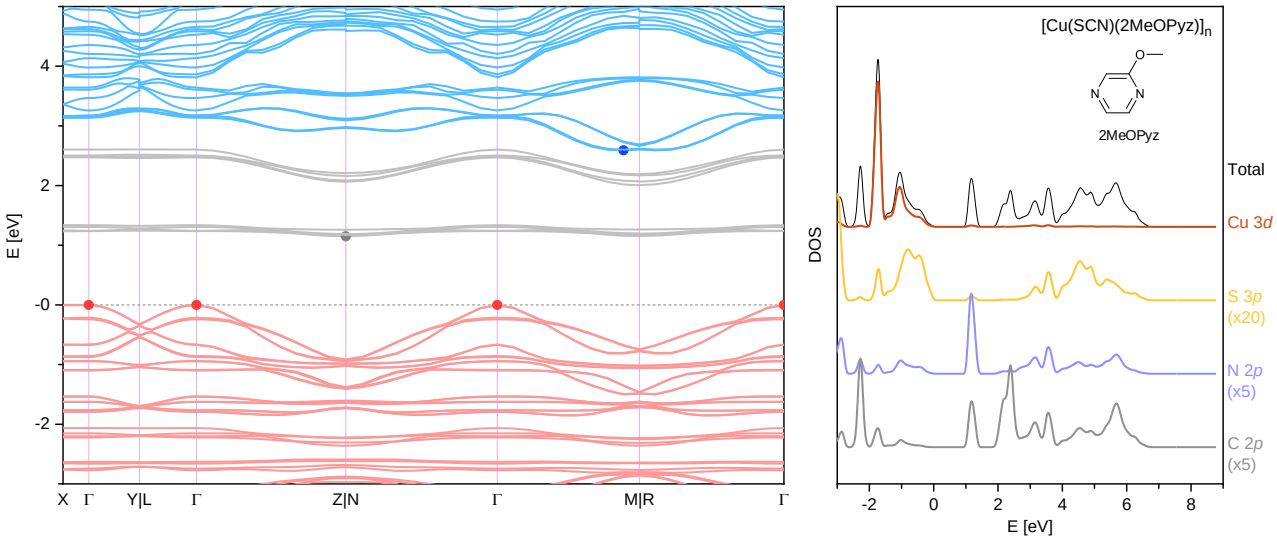

Fig. S9 Electronic band structure and DOS of 2D sheet $[Cu(SCN)(2MeOPyz)]_n$.

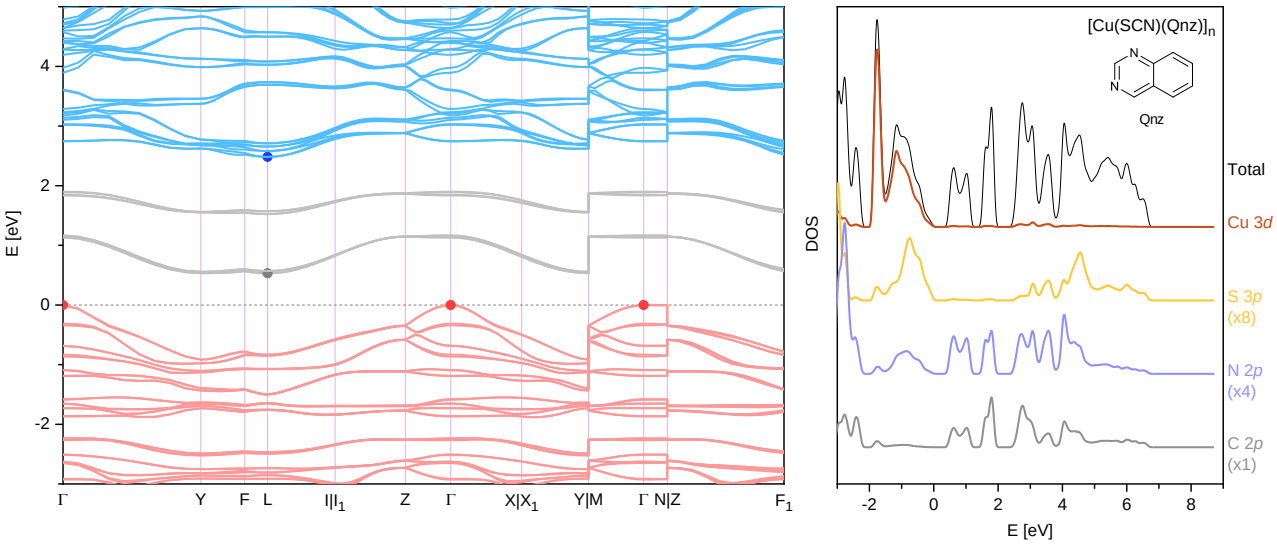

Fig. S10 Electronic band structure and DOS of 2D sheet $[Cu(SCN)(Qnz)]_n$.

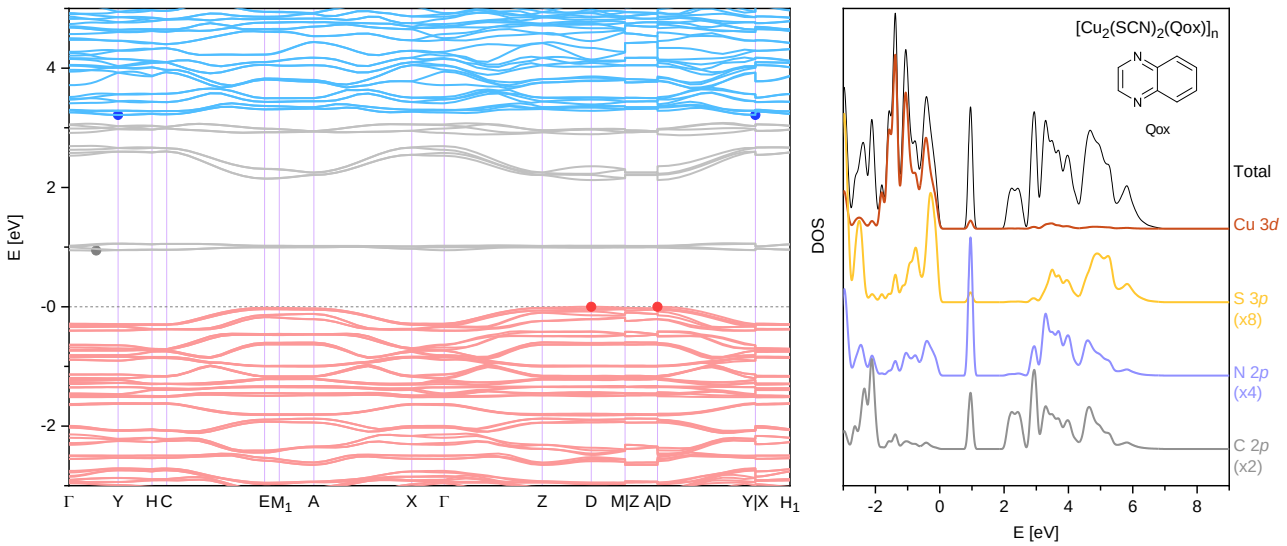

Fig. S11 Electronic band structure and DOS of bridged 1D ladder $[Cu_2(SCN)_2(Qox)]_n$.

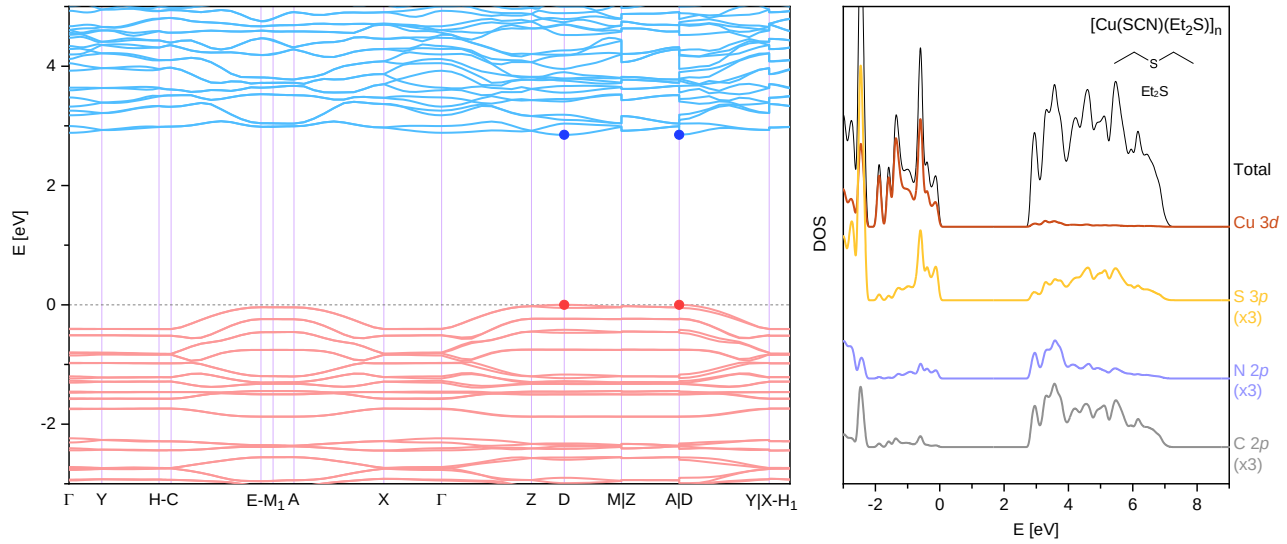

Fig. S12 Electronic band structure and DOS of 1D ladder $[Cu(SCN)(Et_2S)]_n$.

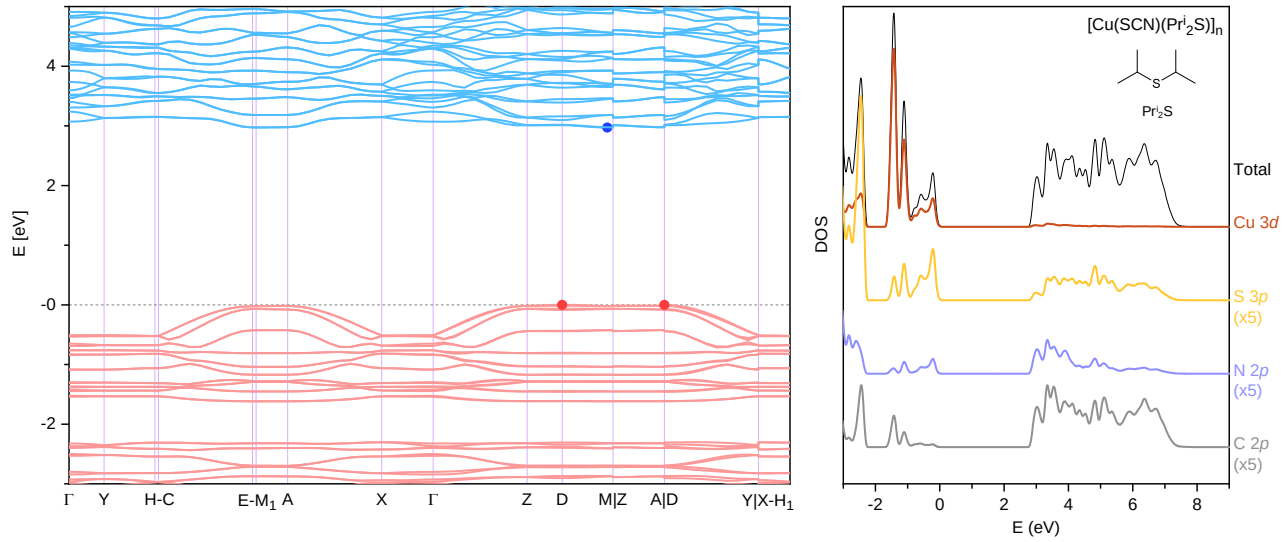

Fig. S13 Electronic band structure and DOS of 1D ladder $[Cu(SCN)(Pr^i_2S)]_n$.

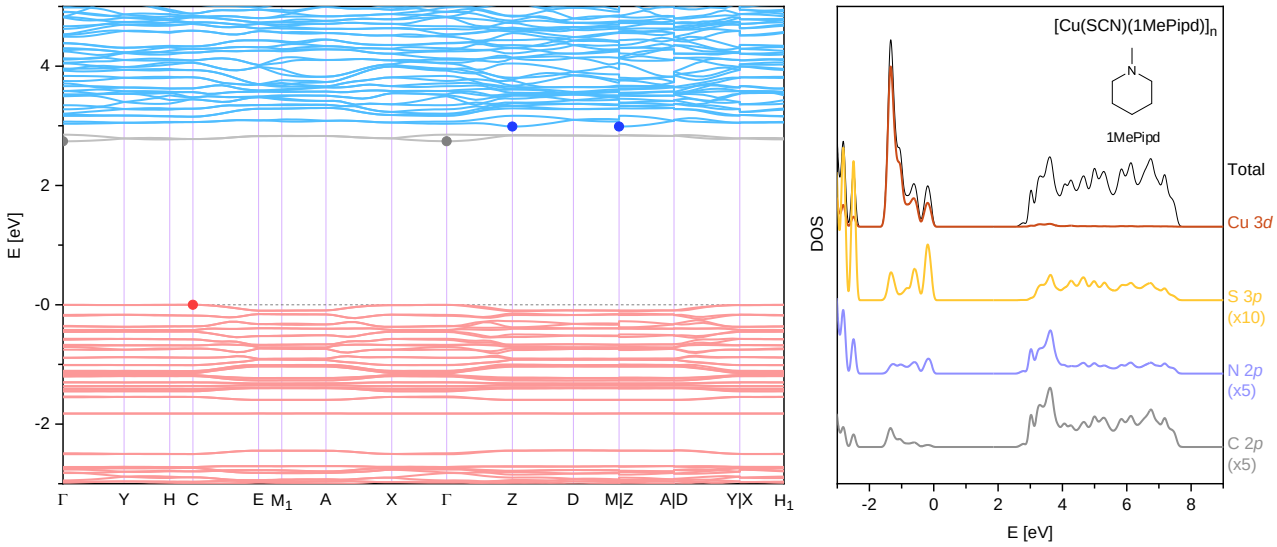

Fig. S14 Electronic band structure and DOS of 1D ladder $[Cu(SCN)(1MePipd)]_n$.

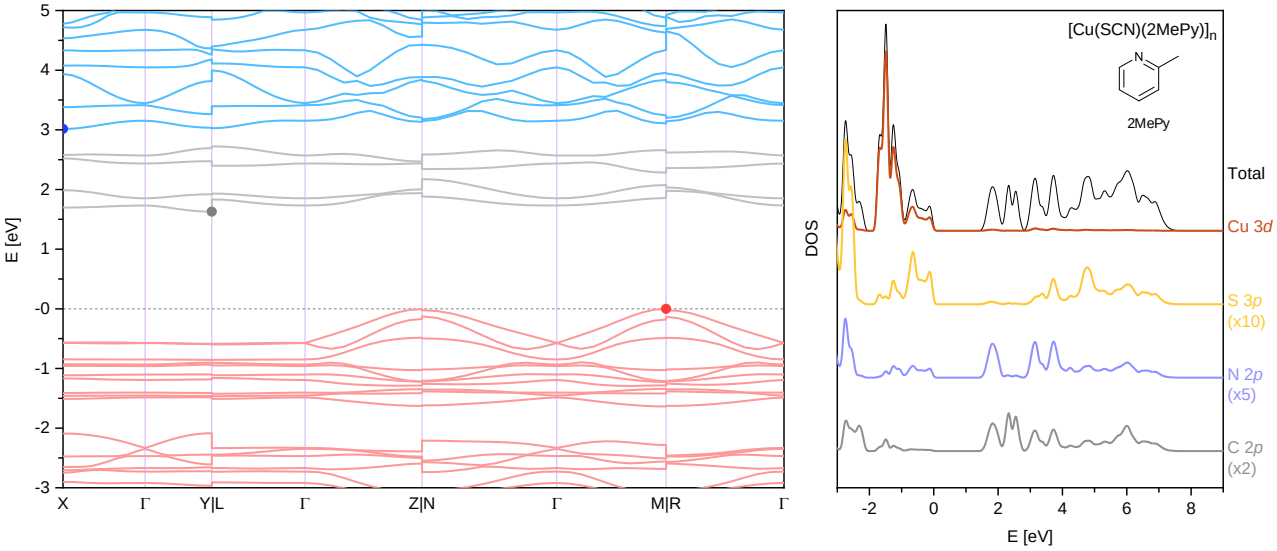

Fig. S15 Electronic band structure and DOS of 1D ladder $[Cu(SCN)(2MePy)]_n$.

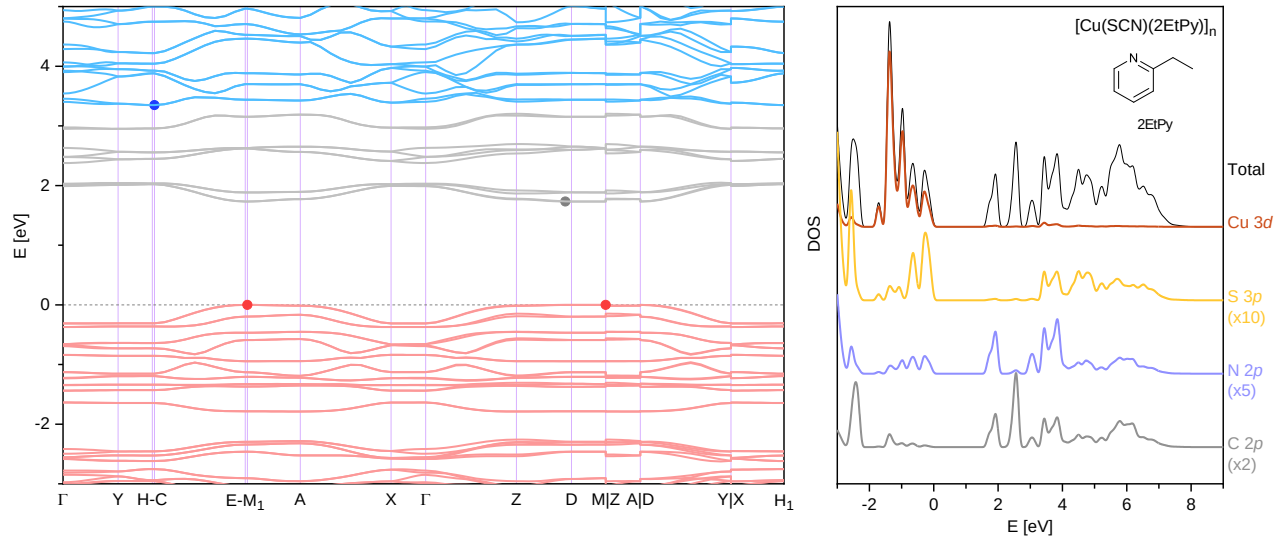

Fig. S16 Electronic band structure and DOS of 1D ladder $[Cu(SCN)(2EtPy)]_n$.

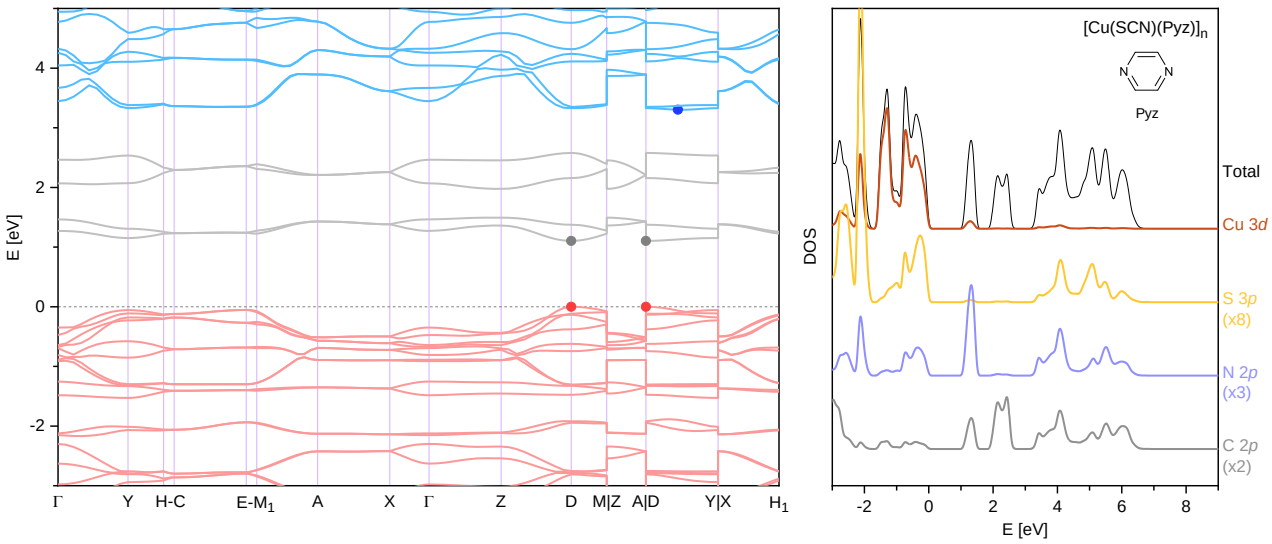

Fig. S17 Electronic band structure and DOS of bridged 1D zigzag chain $[Cu(SCN)(Pyz)]_n$.

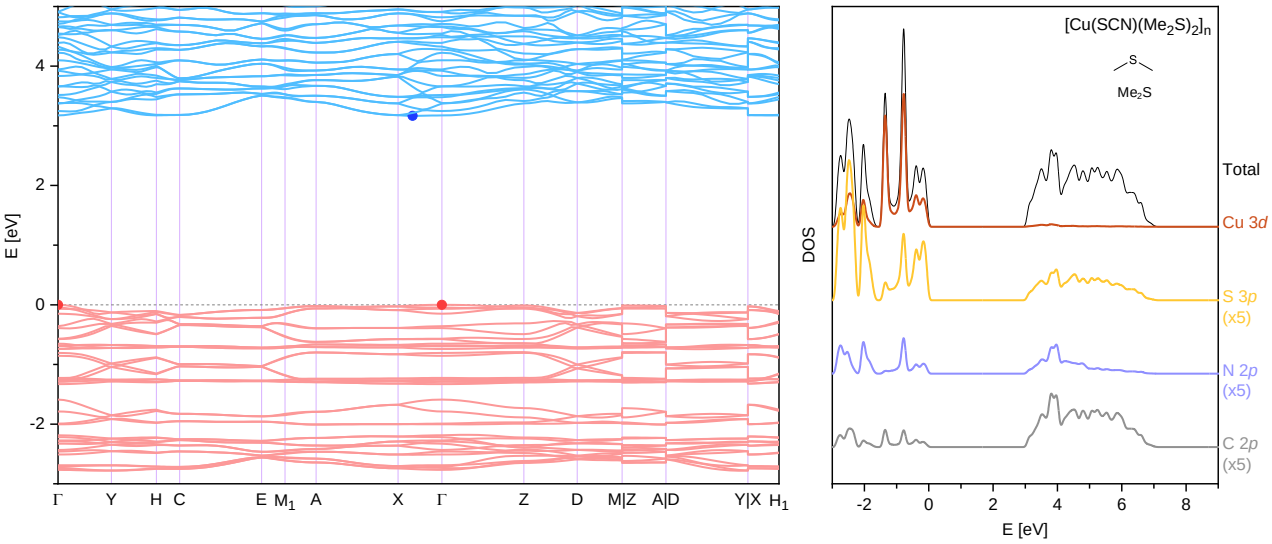

Fig. S18 Electronic band structure and DOS of 1D zigzag chain $[Cu(SCN)(Me_2S)_2]_n$.

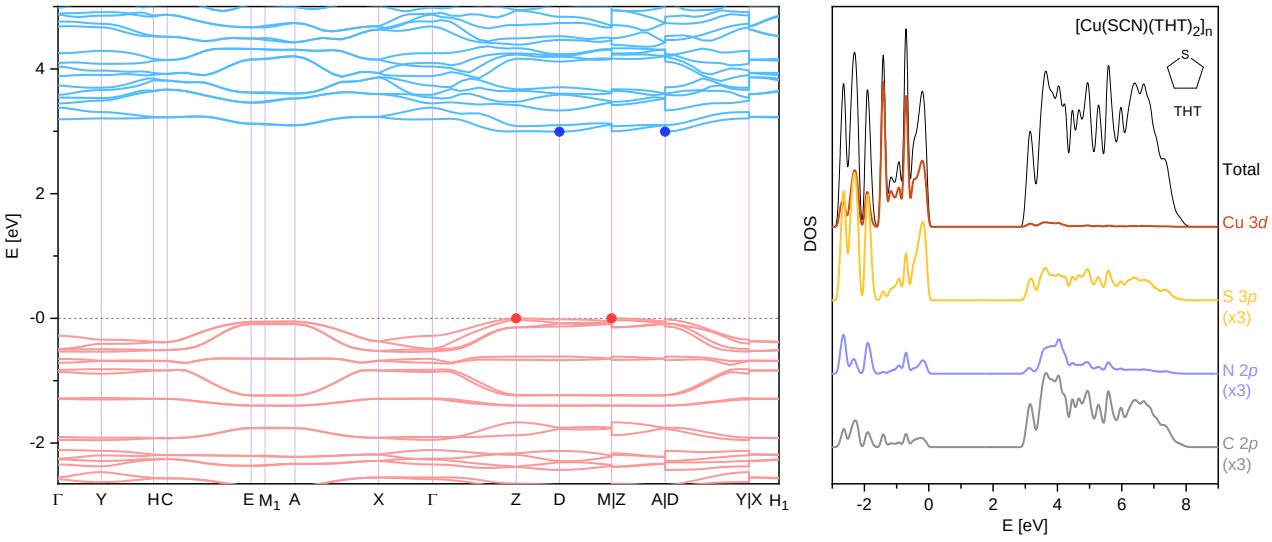

Fig. S19 Electronic band structure and DOS of 1D zigzag chain $[Cu(SCN)(THT)_2]_n$.

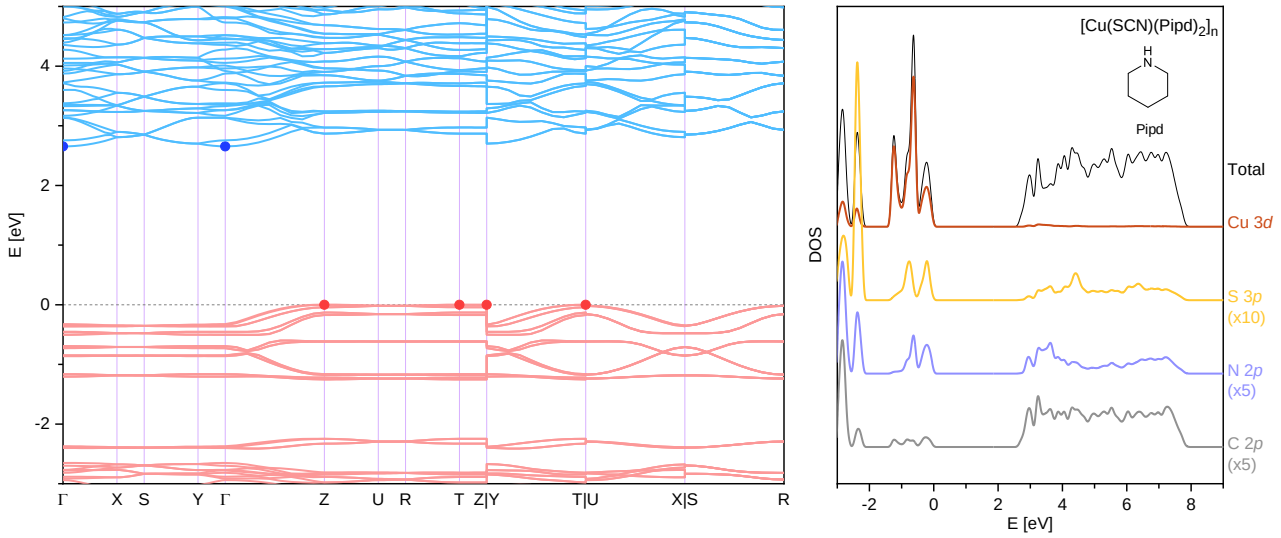

Fig. S20 Electronic band structure and DOS of 1D zigzag chain $[Cu(SCN)(Pipd)_2]_n$.

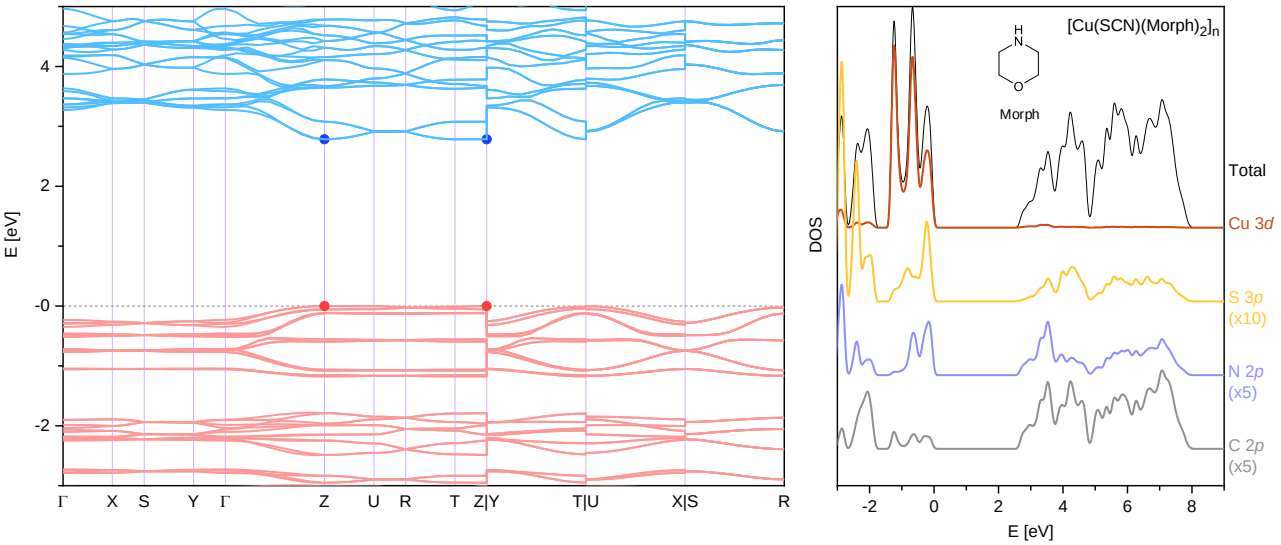

Fig. S21 Electronic band structure and DOS of 1D zigzag chain$[Cu(SCN)(Morph)_2]_n$.

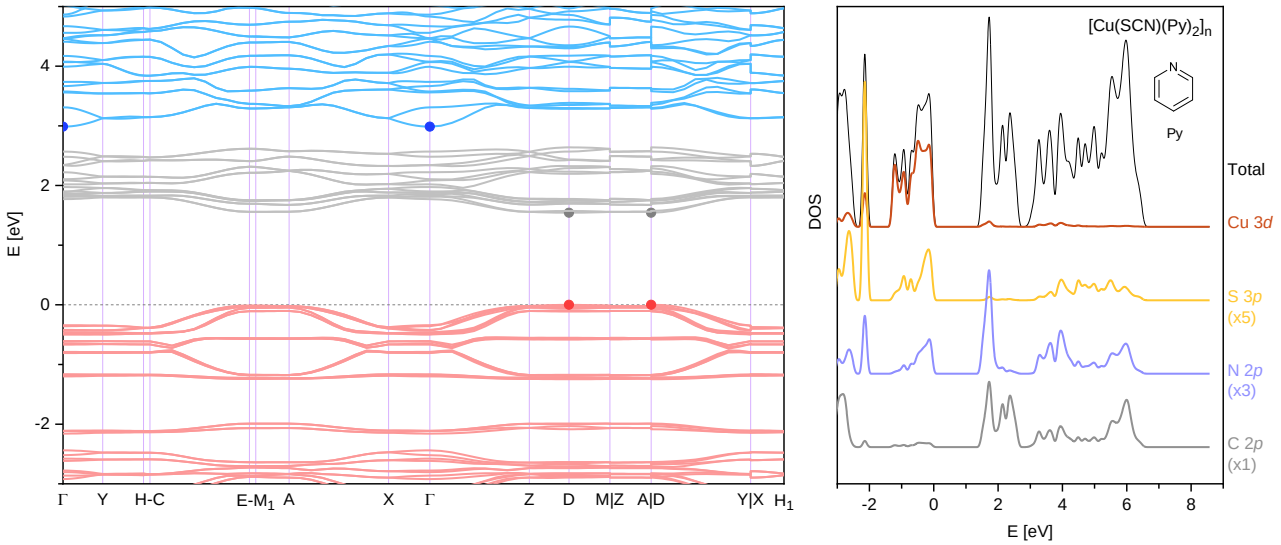

Fig. S22 Electronic band structure and DOS of 1D zigzag chain $[Cu(SCN)(Py)_2]_n$.

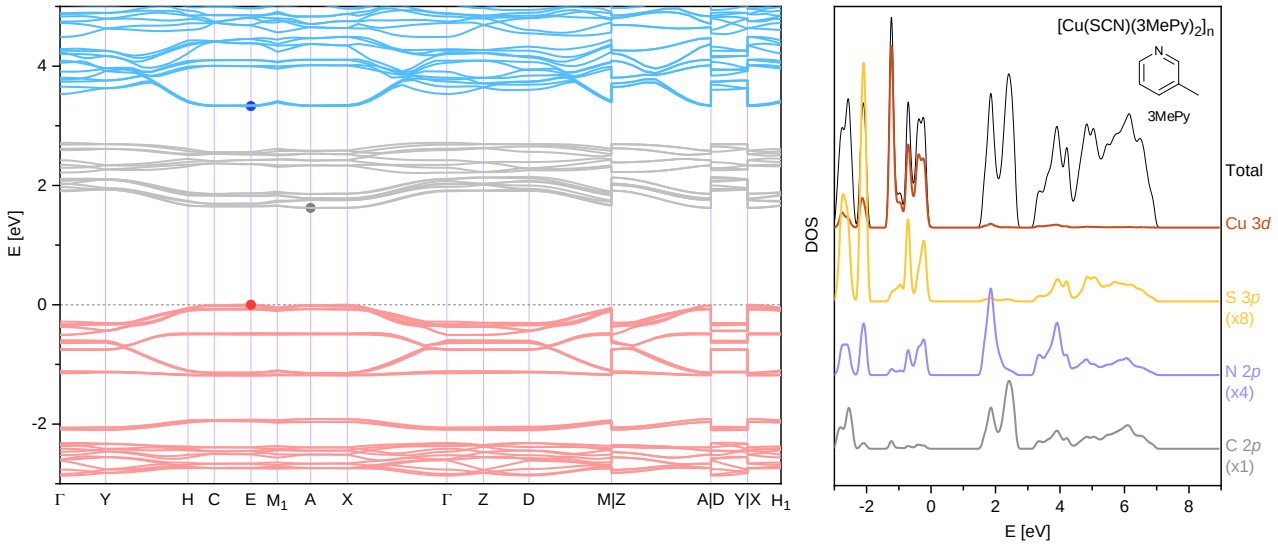

Fig. S23 Electronic band structure and DOS of 1D zigzag chain $[Cu(SCN)(3MePy)_2]_n$.

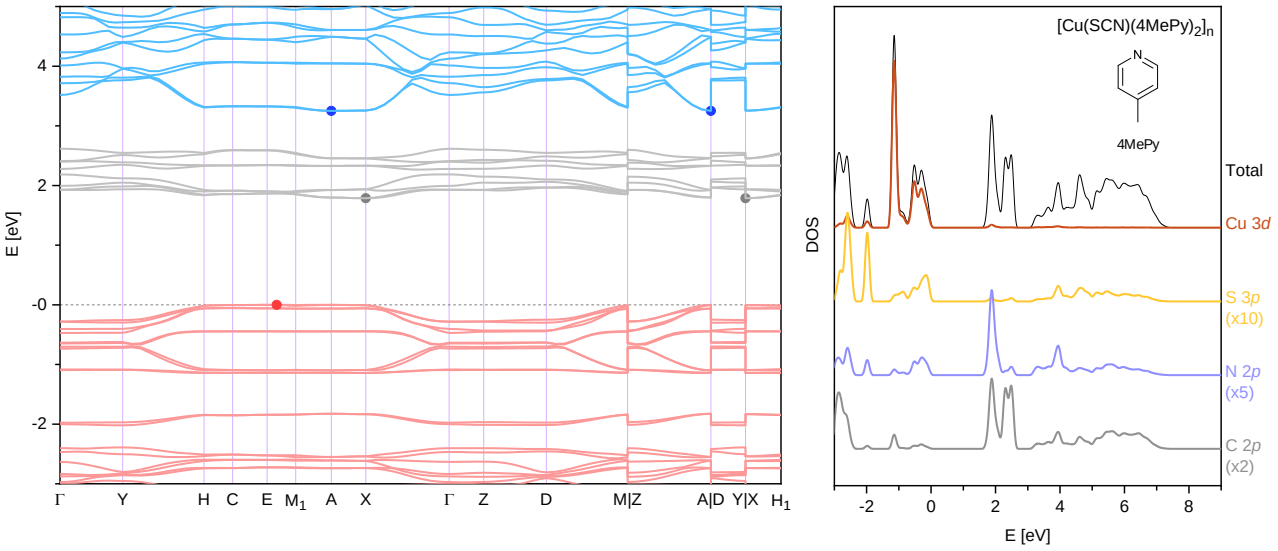

Fig. S24 Electronic band structure and DOS of 1D zigzag chain $[Cu(SCN)(4MePy)_2]_n$.

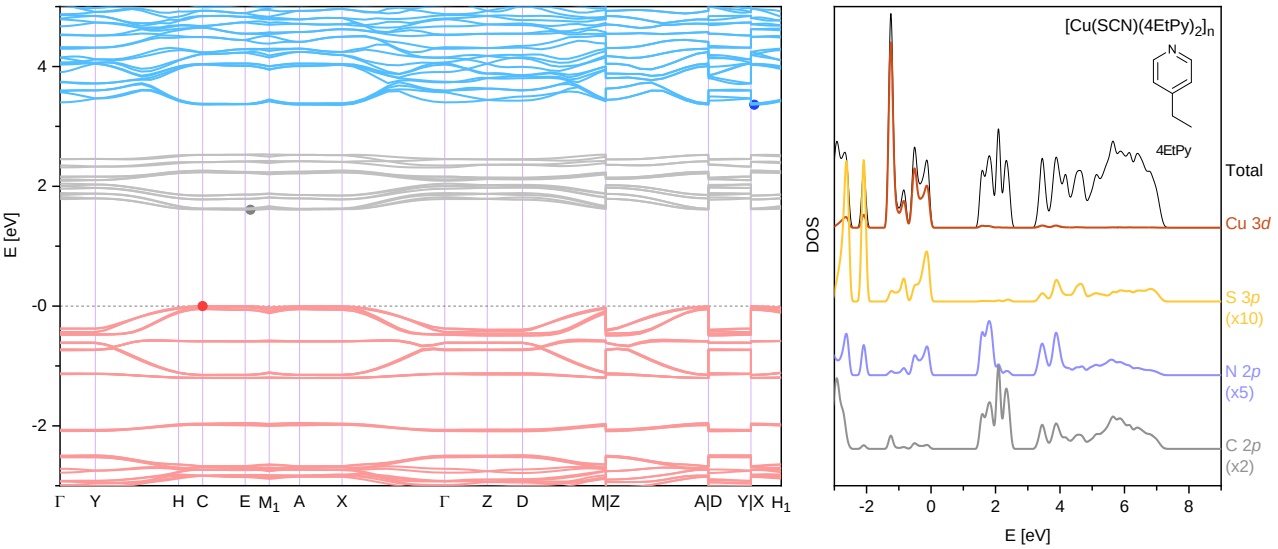

Fig. S25 Electronic band structure and DOS of 1D zigzag chain $[Cu(SCN)(4EtPy)_2]_n$.

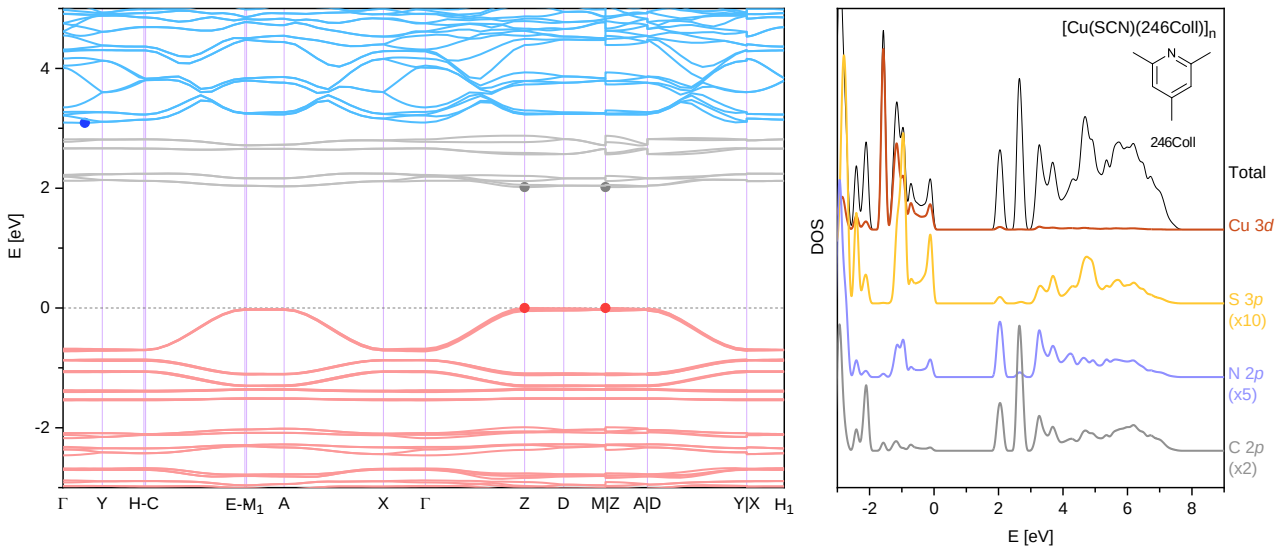

Fig. S26 Electronic band structure and DOS of 1D zigzag chain $[Cu(SCN)(246Coll)]_n$.

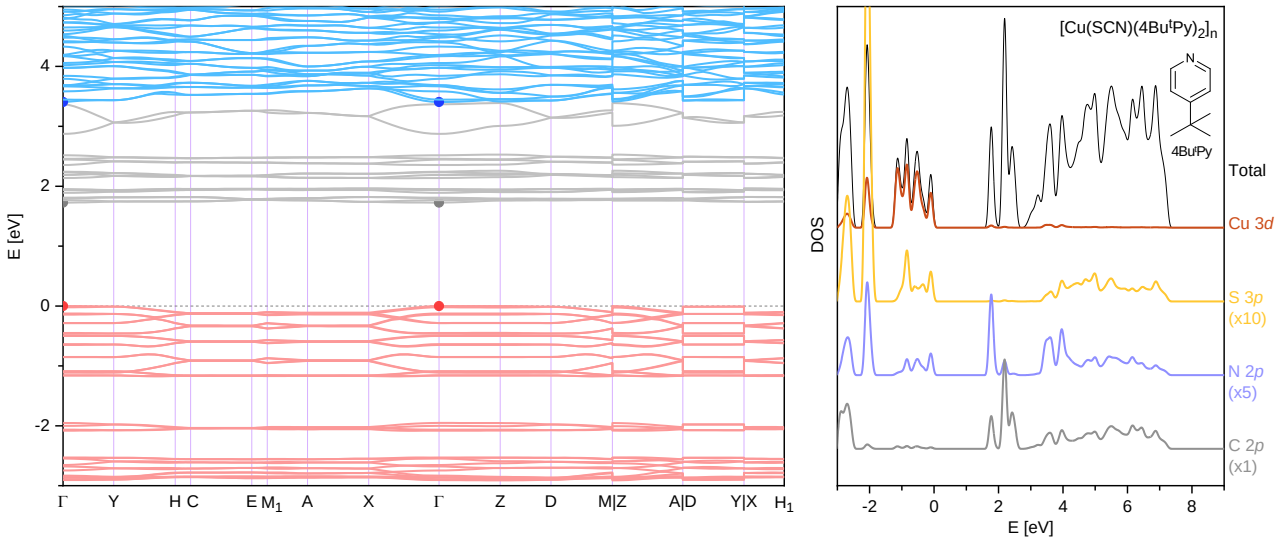

Fig. S27 Electronic band structure and DOS of 1D helical chain $[Cu(SCN)(4Bu^tPy)_2]_n$.

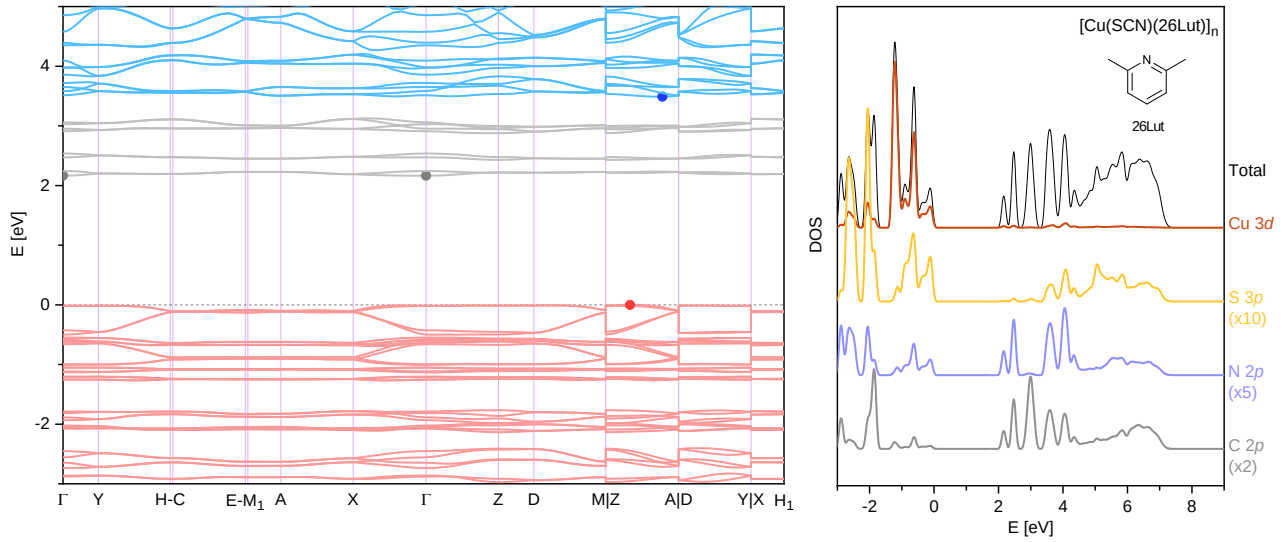

Fig. S28 Electronic band structure and DOS of 1D helical chain $[Cu(SCN)(26Lut)]_n$.

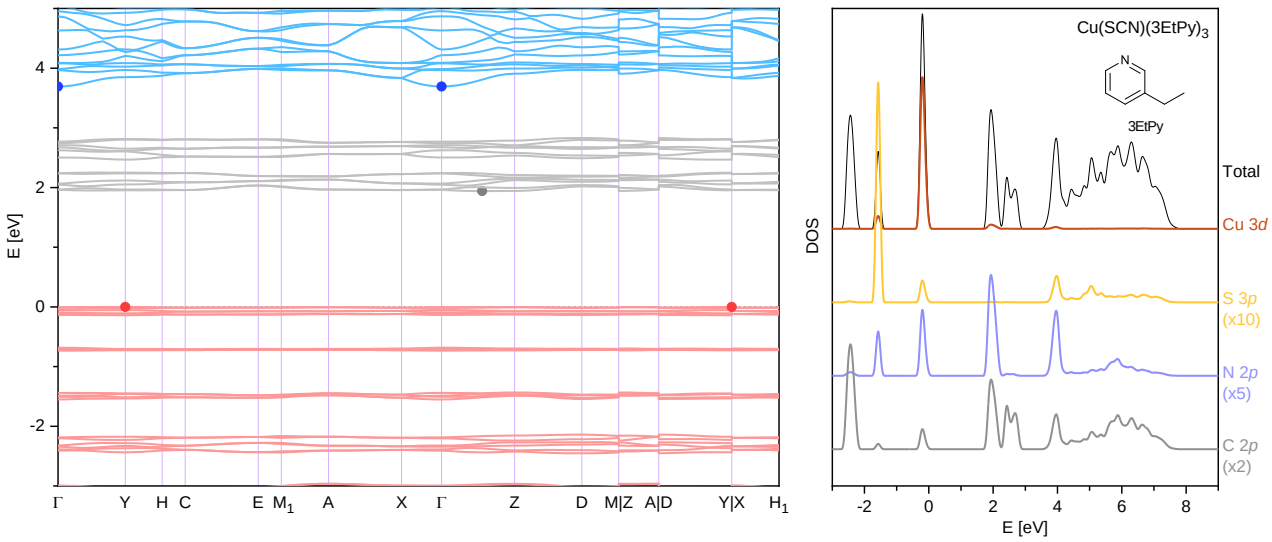

Fig. S29 Electronic band structure and DOS of 0D monomer $Cu(SCN)(3EtPy)_3$.